www.serd.ait.ac.th/reric

Experimental and Prediction of the Development of Low-calorific Swirl Burner

Adi Surjosatyo and Farid Nasir Ani
Fakulti Kejuruteraan Mekanikal
Universiti Teknologi Malaysia
Karung Berkunci 791
81310 Johor Bahru
Johor DT
MALAYSIA

ABSTRACT

This paper discusses the development of swirl vane burner in a staged combustion system. The swirl effect of this burner has benefit to stabilize the flame front and to increase the surface area across in which heat and mass transfer exchange occurs significantly influences heat and mass transfer. Two major methods are used, the mathematical methods using package FLUENT Version 5 and experimental study in a pilot scale of two-stage combustion. There are 3 (three) variation of swirler angle burner model in this investigation i.e. fixed vane swirler with 20, 30 and 40 degree angle (φ) respectively. Measurements of the 20^o, 30^o and 40^o swirl-vane burner flow field and the chemistry in an air staged combustion system has been performed. The predicted and measured flame temperature of each swirl-vane shows a promising result e.g., for application in a small wood dryer.

1. INTRODUCTION

Swirl increases the mixing of fuel and air and has been shown to increase combustion efficiency. It also decreases NO_x emissions in industrial burners and gas turbine engines [1]. Specifically, for methane and natural gas burners, it has been found that the major source of NO_x production is related to the residence time at high temperatures. This means, it is necessary to decrease the amount of time that fluid particles remain at high temperatures. Also, reducing the unmixedness of the fuel and air can reduce NOx. However, it should be noticed that the swirl strength not too high since this could effect the increasing of NO_x emission. According to Gupta et al. [2] since the helical path as the products of combustion leads to a longer residence time at high temperatures with a corresponding increase in NO_x emission. A weak swirl will be no recirculation and the swirling flame will be elongated with an increase the residence time at high temperature. This can encourage the production of NO_x.

The swirl flow effect has usually been used for the combustion and processing of materials that are normally considered difficult to burn or process efficiently such as vegetable refuse, high ash content coals, antracite, high sulfur oils and low calorific value waste gases. Air and fuel are introduced tangentially at one end and combustion takes place, primarily near to the walls, in the swirling flow which spirals along the chamber towards the exhaust at the other end [3]. There exists a high shear and high property gradients in the high turbulence zone at the interface between the jets of fuel and air. It is, therefore, the high heat release rates can be provided by having the regions of high shear stress. The main characteristics of the swirl flow are:

1. Long residence times, which depends upon swirl number and chamber length,
2. A long, thin annular recirculation zone formed internally close to the walls that can be used to enhance flame stabilization,

3. It can be adapted in a two-stage combustor arrangement, the swirl burner type flow in the exit being used to provide an afterburning process which ensures complete fuel burnout.
4. To reduce combustion chamber size by producing higher rates of entrainment of the ambient fluid and fast mixing near the exit nozzle.

Foster et al. [4] have studied some extensive computations of the turbulent combusting flow produced by a burner directed axially into a cylindrical chamber. For combustion flow model they applied a simple one step global methane oxidation reaction mechanism. The mixing rates are determined in terms of turbulent time scale k/ε using relations of Magnussen and Hjertager [5] They have examined two isothermal models: a single equivalent flow and a compound jet flow, in which the fuel and air jet flows are separately represented. The arrangement of the combustion chamber and the burner was considered in figure 1. It shows an inlet flow, which corresponds to the burner and may compromise an individual or a compound flow.

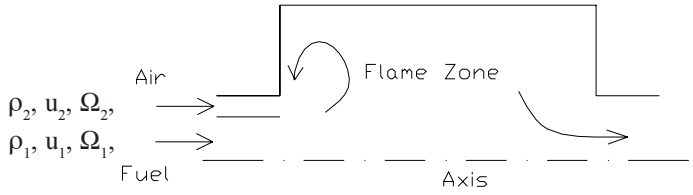

Fig. 1. The arrangement of combustion system used in the computations.

They reported that there are three main recirculation eddies influence the flow: a main outer eddy which was present over nearly the entire range of swirl number, a secondary outer eddy which starts at the chamber corner at zero swirl and an inner recirculation eddy that appears at large swirl. They mentioned also, as swirl number increases the recirculation number mass flow rate gradually decreases, then decreases again at the minimum swirl number, but rises to a peak at large swirl number. They found that the accuracy of representation of the flow in isothermal depends on the swirl number, S and the ratio of the equivalent jet radius to chamber radius, r_e/r_c.

Measurements and predictions of a burner in an unstaged, swirling natural gas flame of 2.25 MW thermal input were conducted by Peters and Weber [6]. Turbulence model was used standard k-epsilon model, and the turbulent combustion model incorporates a two-step reaction scheme together with an eddy break-up model according of Magnussen and Hjertager [5]. In the NO-chemistry model, thermal-NO and prompt NO chemical reaction rates were a statistical averaged using Beta-pdf. The simplified configuration of the gas-firing burner in shown on figure 2.

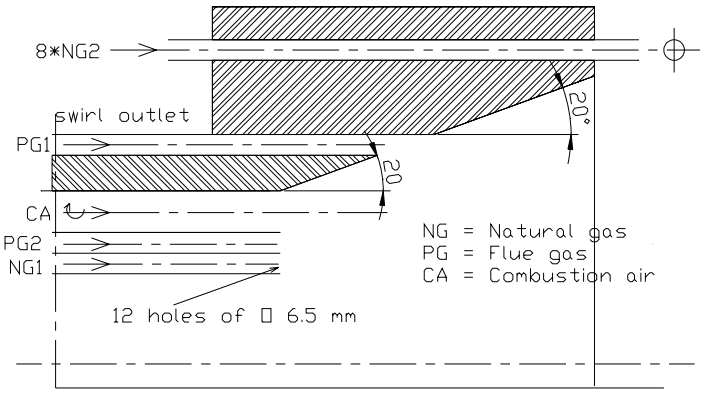

Fig. 2. The configuration of gas-firing burner.

This burner has the inlet swirl number, S_2, of the combustion air stream was 0.6. They reported that the swirl has effected the peak flame temperature and NO_x formation near the swirl outlet. The predicted and measured peak temperatures are 2031K and 2033 K, respectively. However, the temperatures in the shear layer between the flame and the external recirculation zone were affected by the wall temperature.

According to this report, the predicted NO emission varies between 164 ppm and 184 ppm. Compared to measured NO emission, namely, 134 ppm, the prediction is quite good.

The major concern of the present study is to reduce the pollutant emissions, increasing the combustion efficiency and generating the flame stabilization through flow rotation effect. There are 3 (three) variation of swirler angle burner in this study i.e. fixed vane swirler with 20, 30 and 40 degree angle (φ) respectively. These variations are used during simulation and experimental works.

2. SIMULATION PROCEDURE

The Fluent source code release 5.3 is being used to simulate isothermal condition and solving the equations for the mean flow. The turbulence model of the renormalized group theory (RNG) *k*-ε, is two equation models in which the transport equations for two scalar quantities (the turbulent kinetic energy, *k* and its dissipation rate, epsilon-ε) is used to describe the production, diffusion and dissipation of turbulence. The RNG *k*-ε model belongs to the *k*-ε family of turbulence models. Unlike the standard *k*-ε, the RNG *k*-ε model was derived using a statistical technique called renormalization group methods. This model, particularly, has an additional rate-of-strain term in the transport equation ε , so that can provide more accurate prediction of swirl than in standard *k*-ε. When the RNG *k*-ε model was implemented, the swirl dominated flow option was used. This option sets the swirl constant, α_o, 0.35.

2.1 Swirler Gas-Burner Model Geometry

The computational model is applied to the current 3-Dimensional gas burner system and to predict the effect of the different swirler angle of the gas-burner to the flow field of the system. There are 3 (three) variation of swirler angle burner model in this investigation i.e. fixed vane swirler with 20, 30 and 40 degree angle (φ) respectively. These gas burner are parts of the biomass gasifier system. For current work, simplification of the model of gas burner were needed. This means, to simulate these burners, it is not necessary the whole gasifier has to be modeled and simulated. In figure 3 shows the detail configuration of each swirler that are used for the simulation.

2.2. Transport Equations for the RNG k-Epsilon Model

The values of k and ε at the Equation of turbulent viscosity are obtained by solution of conservation energy:

$$\frac{\partial}{\partial t}(\rho k) = \frac{\partial}{\partial X_i}(\alpha_k \mu_{effk} \frac{\partial k}{\partial X_i}) + G_k + G_b - \rho\varepsilon \quad (1)$$

$$\frac{\partial}{\partial t}(\rho\varepsilon) = \frac{\partial}{\partial X_i}(\alpha_\varepsilon \mu_{eff} \frac{\partial \varepsilon}{\partial X_i}) + C_{1\varepsilon}\frac{\varepsilon}{k}(G_k + (1 - C_{3\varepsilon})G_b) - C_{2\varepsilon}\rho\frac{\varepsilon^2}{k}) \quad (2)$$

$$\mu_{eff} = \mu_{mol}\left[1 + \sqrt{\frac{C\mu}{\mu_{mol}}}\frac{k}{\sqrt{\varepsilon}}\right] \quad (3)$$

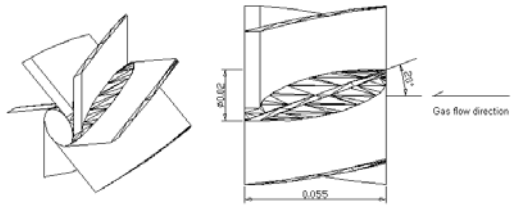

(a) 20^{O} swirler vane-pack

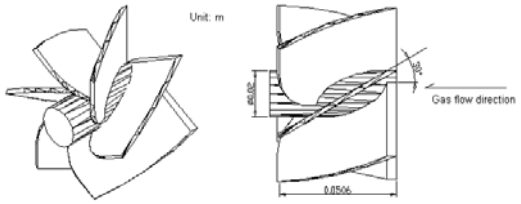

(b) 30^{O} swirler vane-pack

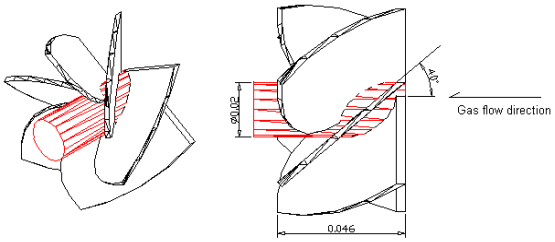

(c) 40^{O} swirler vane-pack

Fig. 3. Configuration of different swirler turning vane pack (20^{O}, 30^{O}, 40^{O}).

2.3. Reacting Flow

This model was implemented on the burner-nozzle zone, because the premixed of gas mixture occurred before entering the burner-nozzle. Solving this reaction, the methane combustion modeling is necessary simulated by a two-step chemical mechanism. The methane two-step combustion model consisted of the following reactions:

$$CH_4 + 1\,½\,O2 \Rightarrow CO + 2\,H_2O \quad (4)$$

$$CO + ½\,O2 \Rightarrow CO_2 \quad (5)$$

Rate expressions for the forward reactions are generalized in Arrehenius form, based on reactant concentrations [R_i] and temperature T:

$$R_{ef} = -\nu'_{i,k} A T^{n} [R_a]^{a} [R_b]^{b} \exp\{E_A/RT\} \quad (6)$$

where $-\nu'_{i,k}$ is molar stoichiometric coefficient for species *i* in reaction k (*positive* values for reactants, *negative* values for products), A is pre-exponential factor (consistent units), T is temperature (K), n is temperature exponent (dimensionless), *a* and *b* are species exponents and E_A is activation energy for the reaction (J/kmol). Table 1 lists the reaction rate constant used in this study.

The influence of turbulence time scale k/ε on the reaction rate was taken into account by employing the Magnussen and Hjertager model [5]:

$$R_{Rk} = -4\nu_k M_i \rho \varepsilon/k \frac{m_r}{\nu_r M_r} \quad (7)$$

$$R_{Pk} = 2\nu_k M_i \rho \varepsilon/k \frac{\sum_P m_P}{\sum_P \upsilon_P M_P} \quad (8)$$

The model is applied, without modification, to the combusting. This gives a consistent representation of the flow and combustion physical processes and the comparisons between two cases should be insensitive to the particular turbulence and combustion models employed.

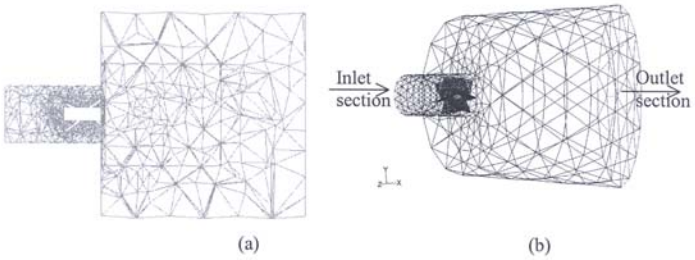

Fig. 4. Typical of the computational mesh pattern of the swirler burner (20° vane pack).

The computational model on which the present investigation of isothermal modeling is given as follows. The current model is apart of gasfier system, therefore, to simplify the simulation, not the whole component is performed. Only the swirler burner part will be performed. A computational mesh pattern of this swirler burner is constructed in figure 4.a and 4.b. These show the mesh pattern which sufficient to this model was built multi-block mesh, i.e. triangular and quadrilateral mesh. This geometric model was considered to make use of the advanced gridding capabilities of FLUENT and to represent the geometric as closely as possible The volume of final geometry of each burner is divided into 24543 triangular faces, 11507 tetrahedral cells and 2696 nodes.

2.4 Boundary Condition

Calculations were performed here for the full-scale of nozzle-burners and were carried out for methane/air velocity of 29 m/s at inlet temperature of 420 K and a pressure of 760 mmHg (1 bar). The other properties such as density, viscosity, ambient pressure etc. was at condition of inlet temperature of 420 K. Typical of Reynolds number are of the order of 10^5. Buoyancy effects are assumed to be negligible. The inlet mass fractions of CH_4 was 0.0001466, O_2 : 0.12, CO_2 : 0.11, CO: 0.004431, and H_2O : 0.01 of mass fraction, respectively. Relationships for fully developed turbulence were applied at the inlets to determine k, ε and the Reynolds Stresses components.

The eddy breakup model relates the rate of reaction of dissipation of the Reactant (R) and Product containing eddies, k/e represents the time scale of the turbulent eddies following the eddy breakup model of Spalding [7].

3. EXPERIMENTAL SET-UP

The current swirl burner is the upper part of the complete combustion system that was fabricated in the combustion laboratory. Figure 7.a and 7.b show the configuration of the combustion system and

enlargement of secondary chamber, respectively. Table 2 presents the important parameter of the current designed swirl-vane burner. The fuel-gas in the gas burner is produced by the gasifier, the lower part of the combustion system.

Table 1. Reaction Rate Constants

	Reaction 1 (Eq. 4.5)	Reaction 2 (Eq. 4.6)
Arrehenius Pre-Exponential Factor, A	5.012e+11	2.239e+12
Activation Energy, J/kmol	2e+8	1.7e+08
Rate exponent for CH_4	0.7	-
Rate exponent for O_2	1	0.25
Rate exponent for CO	0	0
Rate exponent for H_2O	0	0.5
Rate exponent for CO_2	0	0
Temperature exponent, n	0	0

Table 2. Parameter or Dimension of Fabricated Burner

No.	Vane angle (φ)	Number of vane	Dimension of the swirl-vane (l,w,th,d, d_h) in mm					Swirler Number (S)
			l_e	w	th	d	d_h	
1	20	6	53	35	1	83	19	0.22
2	30		50.6	33	1	83	19	0.356
3	40		38	31	1	83	19	0.508

where l_e is equal length of vane, w is width of vane, th is thickness of vane, d is circle diameter of vane and d_h is hub diameter of vane.

The producing gas from the primary chamber was kept constant around 0.64 gr/min. For the secondary air, its flow rate was varied from 438, 498, 535 and 622 lpm. The operating conditions for the turbulent premixed flames considered in the present study are summarized in table 5.2. The nominal heat release rate is obtained by multiplying the fuel mass flow rate by its nominal heating value of 5100 kJ/kg [8].

Table 3. Operating Conditions for Turbulent Premixed Flames

Flow Parameter	Swirl-vane angle		
	20^o	30^o	40^o
Equivalence Ratio, -	1.16 – 1.66		
Nominal heat Release, kW	5.8		
Gas flowrate, g/hr	1.04		
Flame Temperature, ^oC	560	569	632
Temperature at burner exit, ^oC	244	253	284
Range of secondary air flowrate, lpm	438 – 622		
Combustor pressure, atm	Atmospheric pressure		

3. Instrumentation Set-Up

The flowmeter used was ventury type and before utilized for the air flowrate measurement (primary and secondary air supply), it was calibrated with the standard flowmeter. Adjusting the air supply consumption, two air valves were mounted on each air-supply pipes. Measuring the air flowrate can be done directly through reading the differentiation of water level in the U-tube.

Temperature distribution were detected by Chromel- Alumel Thermocouple K-type assembly. There are six thermocouple-probes located inside the primary-chamber. They are placed inside the reactor in such away that their tip remains along the axis of the chamber. The distance between the thermocouples was determined to ensure the best description of the temperature field along the axis and to allow for an accurate determination of the propagation velocity of the combustion front.

Another thermocouple-probe in the cyclonic chamber and three probes in the secondary chamber. All these thermocouple-probes connected with a system data-logger from Data Taker 605 and all the data by the computer displayed online.

A Rosemount Series 500 gas-analyzer allows to follow discontinuously the concentration of O_2, CO, Nox, CO_2, Excess-air, and Combustion Efficiency. When measured all the data the gas-probe tip was inserted into the secondary chamber.

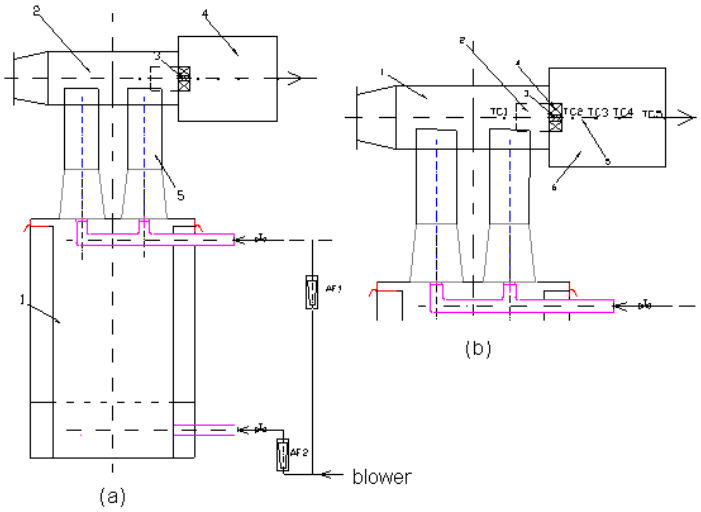

Figure 5. (a) The configuration of the combustion system with, 1: Primary chamber, 2: Cyclonic chamber, 3: Swirl vane, 4: Secondary chamber, 5: Gas ejector.

(b) The enlargement of secondary chamber with, 1: Cyclonic chamber, 2: burner tube, 3: Vane-hub, 4: Swirl vane, 4: Secondary chamber, 5: Flame zone.

4. RESULTS AND DISCUSSIONS

4.1 Effect of Different Swirler-Vane Burner Configuration on Combustion Emission

Figure 6.a. shows the decay of predicted carbon dioxide in the axial direction. In general, the reaction process occurs slowly starts before entering the swirl-vane, this condition is indicated by the rising of the temperature from 487.7 to 853 K as shown in figure 7.a.

After leaving the swirl-vane, CO_2 rises quickly due to the flame velocity increasing in this region. On the same time the temperature reach their peak values i.e 987.74 K for 20°, 963.92 K for 30° and 917 K for 40° swirl-vane, respectively.

In this region develop a high mixing process and reaction kinetic rate that are caused by developing RFZ, CTRZ and PVC structure. These structures are the important factors in swirling combustion in related to increase the overall combustion efficiency and reducing the pollutants without increasing the combustion temperature.

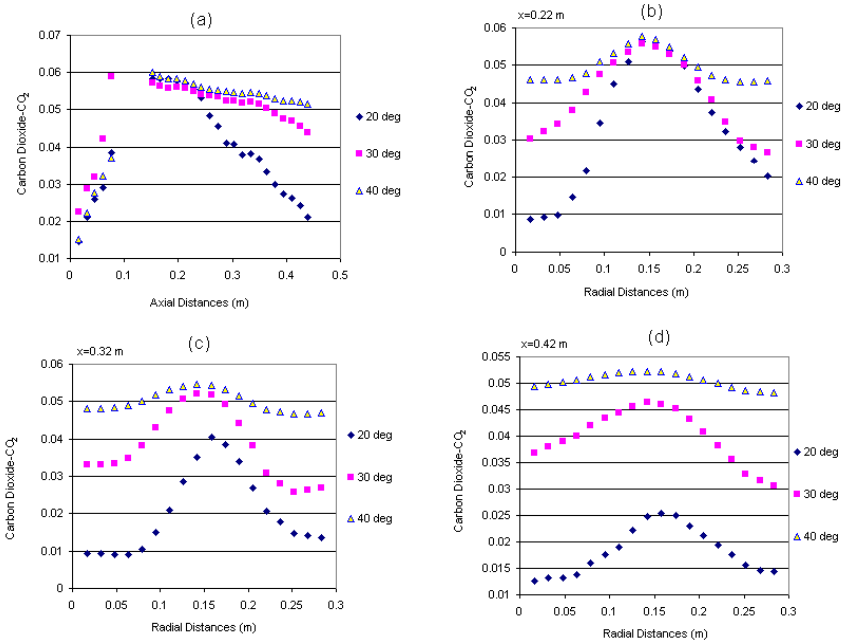

Fig. 6. Effect the variation swirler-vane angle to the predicted carbon dioxide (CO_2) distribution in axial (a) and radial direction (b, c, d).

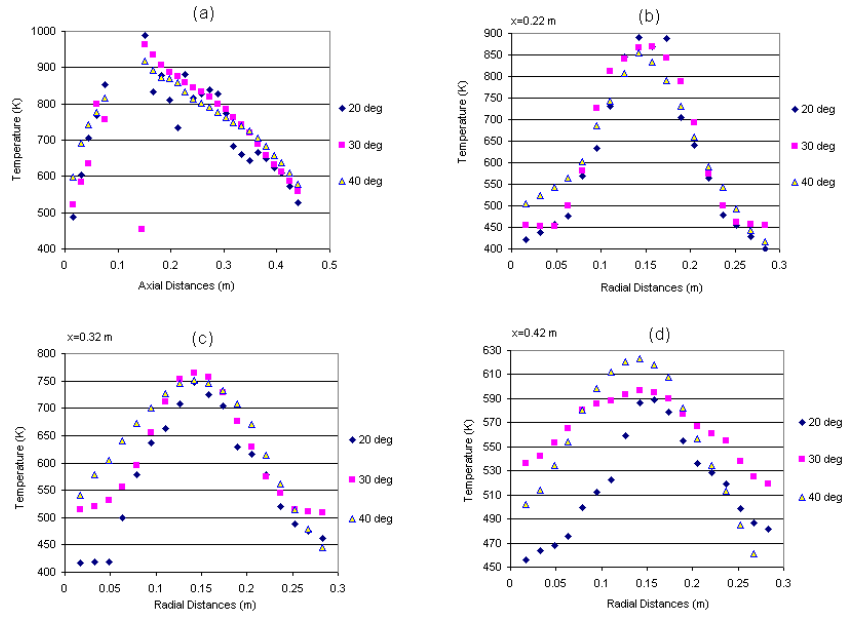

Fig. 7. Effect the variation swirler-vane angle to the predicted temperature distribution in axial (a) and radial direction (b, c, d).

Figure 6.b to 6.d show the variation CO_2 level at different plane of x = 0.22 m, x = 0.32 m and x = 0.42 m. In the center of swirl burner due to the effect PVC structure, the CO_2 has a high emission level, than it decays when the radial distance rises. In PVC structure, which occurs in burner central, there is a high potential tangential velocity that cause high kinetic rate. Thus, it appears this kinetic rate produces high combustion temperature. A higher methane combustion rate as result of the effective mixing with the oxygen consumption produces a lower Unburnt HydroCarbon (UHC) as depicted in figure 8.a and 11.a.

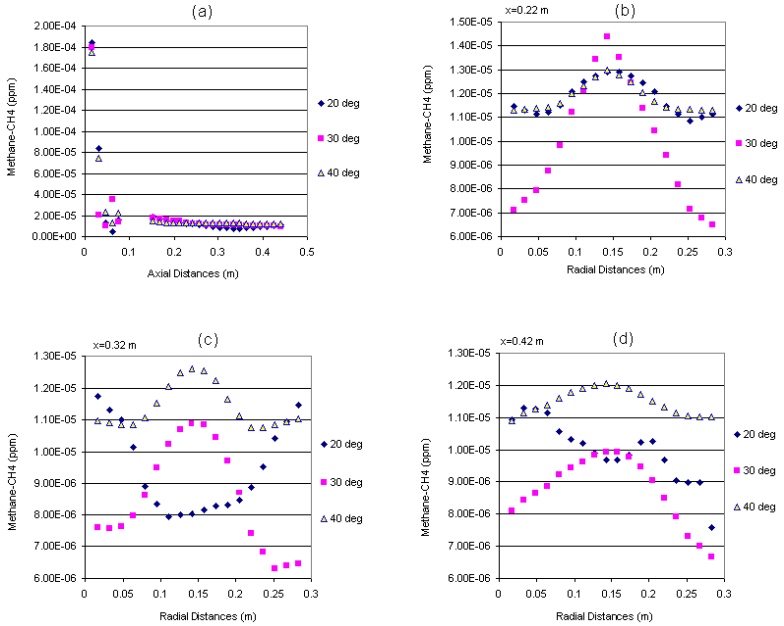

Fig. 8. Effect the variation swirler-vane angle to the predicted methane distribution in axial (a) and radial direction (b, c, d).

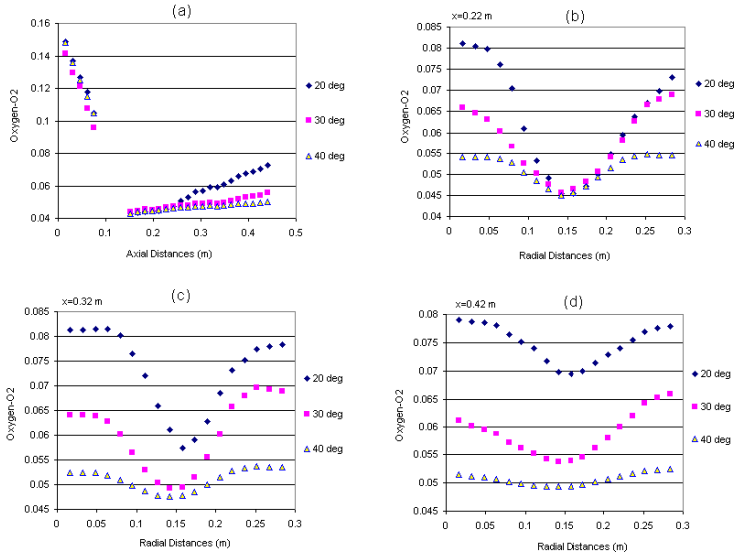

Fig. 9. Effect the variation swirler-vane angle to the predicted oxygen (O_2) distribution in axial (a) and radial direction (b, c, d).

The region where the combustion takes place, the oxygen consumption is also high and then it decays along the burner chamber as plotted in as plot in figure 9. However, the CO emission level appears high enough in this region. It is caused by the effect very fast combustion process, so that the char particle does not react completely with the oxygen. After increasing the Oxygen content due to the reducing combustion intensity, there is an enough time to complete the reaction so that the CO level can be reduced properly.

Figure 10. b to 10.d show the radial distribution of CO concentration on each swirl-vane angle. As already mentioned at the previous paragraph, the CO concentration is very dependent on the Oxygen variation. In the center of the burner chamber, since the Oxygen is needed for burning the char, the CO production is high. Increasing the radial distance away from the center region, the oxygen level rises slowly then reacts to the rest of the char to complete the reaction process. The result is the reduction of CO concentration significantly.

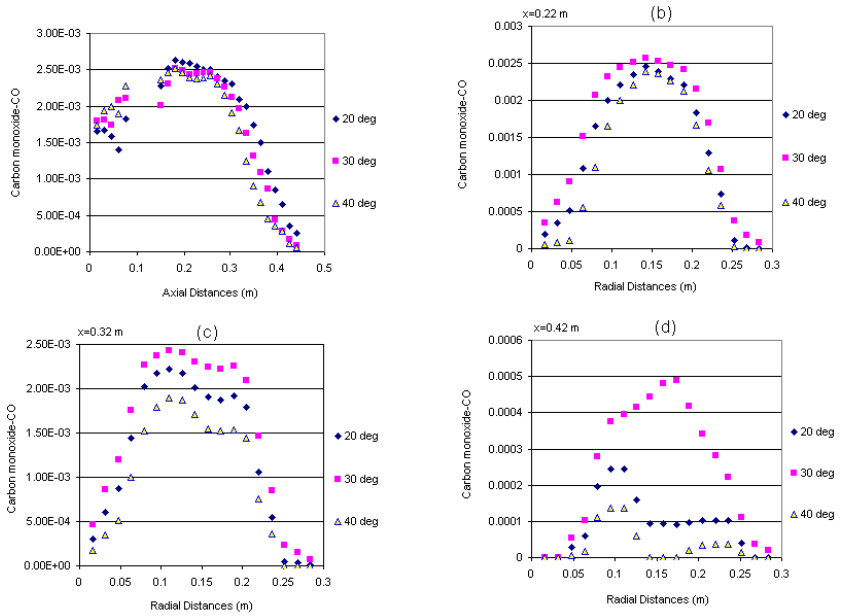

Fig. 10. Effect the variation swirler-vane angle to the predicted carbon monoxide (CO) distribution in axial (a) and radial direction (b, c, d).

4.2. Comparison with the Experimental Results

Figure 11 shows the temperature comparison between the prediction and experimental study. In general, the experimental result gives the similar trend with the predicted result. The maximum temperature of both curves, occurs at the same zone of the swirl burner centerline, i.e. at x= 0.16 to 0.24 m. The predicted temperature results of 20^o and 30^o indicate an over prediction of 26.5 % and 21.3 %, respectively, close the swirl-vane exit. While for 40^o is almost agree with the experimental result with different results of 1.9 %. It is possibly, for 20^o and 30^o occur a higher local turbulence intensity, as consequence gives more complex combustion process that may produce radiation and convective heat near the swirl-vane exit. These conditions could create difficulties to predict accurately. However, for 20^o and 30^o swirl-vane, as plotted in figure 11.a and 11.b, the predicted curve could approach the real condition. The curve of the predicted temperature is fluctuate at the distance of x= 0.16 to 0.24 m. Beyond this distance, the predicted temperatures decay are slightly above the measurement result.

Since combustion process is the complex behaviour, is difficult to predict precisely. It has the possibility that the effect of radiation model, P1, fails to predict accurately. The radiation factors that

given in boundary condition, such as wall thickness of the burner and heat transfer coefficient, possibly have not effected too much to the result in this zone.

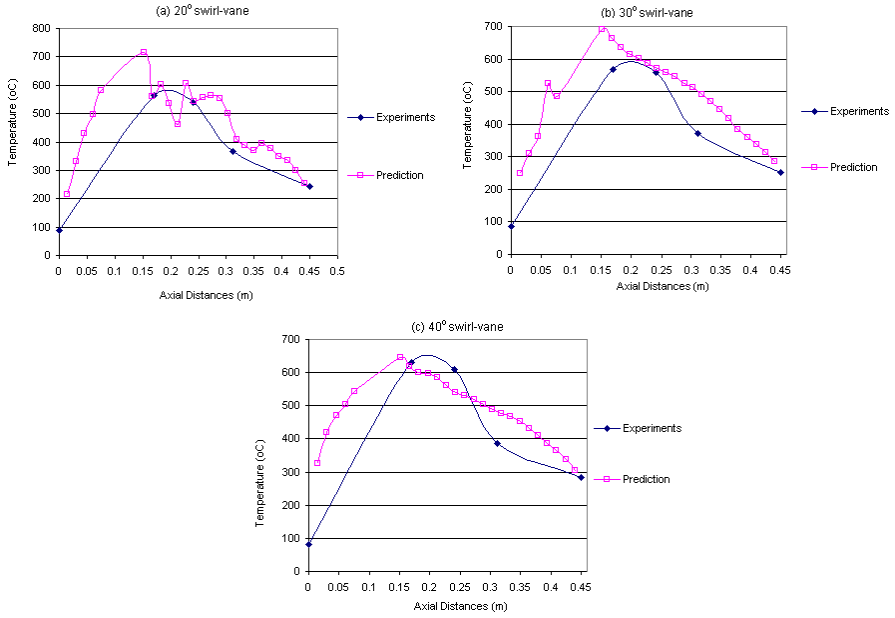

Fig. 11. Comparison the predicted temperature with the experimental results for different swirl-vane angle at $\phi = 1.33$.

Table 4 shows other comparison the predicted and experimental results at the burner exit with $\phi = 1.33$ for each swirl-vane angle burner. The CO_2 emission in volume gives overpredicted results for 30° and 40° swirl-vane due to the predicted temperature give the overprediction results. The aerodynamic effect of the swirl vane and in the same time occurs the combustion process effects to the high CO_2 formation in predicted result. Furthermore, this influences to encourage a higher combustion temperature. As consequence, the predicted O_2 in the reaction is more consumed and therefore lower than measurement results. The deviation of predicted O_2 are dependent also to the deviation of predicted temperature, which give overpredicted value of 3.7 % for 20° swirl-vane, 11.41 % for 30° swirl-vane and also overpredicted of 6.63 % for 40° swirl-vane.

The higher predicted temperature effects to the underpredicted of CO of 40.71 % for 30° swirl-vane. The 20° and 40° swirl-vane shows the overpredicted and underpredicted of 9.2 % and 18.2 % respectively.

Table 4. The emission comparison of prediction and experimental results of all swirl-vane at the burner exit

EMISSION	SWIRL-VANE ANGLE								
	20°			30°			40°		
	Pred[1)]	Expr[2)]	%Error	Pred[1)]	Expr[2)]	%Error	Pred[1)]	Expr[2)]	%Error
CO_2 (% vol)	7.2	13.7	-47.44	21.6	14.4	+50.27	19.3	14.6	+32.4
O_2 (% vol)	6	6.2	-3.22	5	6.5	-23.84	5.1	6.2	-18.38
CO (ppm)	250	227	+10.13	167	235	-28.93	55	65	-15.38
NO_x (ppm)	237.8	260	-8.53	115.3	210	-45.10	82.9	70	+18.43
Temperature (°C)	253.5	244	+3.87	285.6	253	+12.88	304.2	284	+20.18
Average η_{CE} (%)	81.2	73.6	+10.27	83.8	76.9	+6.86	93.3	95.1	-1.94

5. CONCLUSIONS

Measurements and predictions of the 20°, 30° and 40° swirl-vane burner flow field and the chemistry in an air staged combustion system has been performed. The applied mathematical models for prediction of velocities, turbulence quantities, temperature and chemical species concentrations of hydrocarbons, carbon monoxide, oxygen, carbon dioxide and nitride oxide have been described and discussed in detail. Turbulent combustion has been modeled by means of the eddy break-up concept. A comparison between measurement and predictions of biomass gas flame in different swirl-vane angle has been carried out.

Increasing of the swirl-vane angle correlated with the increasing of swirl number, *S*. Computationally investigation has given the significant development of CTRZ volume when the swirl number increase. The CTRZ is developed in the central region of the jet close to the swirl-vane exit. The boundary of the recirculation is determined from the radial points at which the reverse flow rate equals the forward at the axial position. The CTRZ associated with the high swirl is beneficial to fuel mixing, ignition and flame stabilization. The recirculating flow generates regions of high turbulence intensity between the forward and reverse flow, resulting in faster mixing of combustion air with fuel. Furthermore, a higher swirl number, means higher of PVC frequency that can give increase tangential velocity and impact to a higher capability of the flame stability.

The predicted and measured flame temperature of each swirl-vane shows a promising result. For further research, this type of burner can be applied in a small wood dryer. Event though the 20° swirl-vane gives the highest discrepancy i.e. an overprediction of 20.1%, the all curves indicate a similar trend. The CE (η_{CE}) shows a good agreement with the experimental result and in same time the combustion system can give a high combustion of hydrocarbon. The overall agreement between predicted and measured CO, O_2, and CO_2 concentration in the flame zone is found to be also good. This is with the exception of the fact that, for 30° swirl-vane is resulting underpredicted predicted CO emission with a high of 40.71%. A possible explanation for the observed discrepancy between prediction and measurements is believed to lie in the fact that the design model of 30° swirl-vane exist a rounding that close to the hub.

6. ACKNOLEDGMENT

The authors are grateful to the Ministry of Science, Technology and Environment under the IRPA Research Program for research grant awarded and Combustion Laboratory Universiti Teknologi Malaysia for the support during carry out the research work.

7. NOMENCLATURES

A_1, A = pre exponential factor, -

c_p = heat of capacity, *J/kg.°C*

$C\mu$ = empirical constant 0.0845

CTRZ = Centre Toroidal of Recirculation Zone

d_0 = jet diameter, m

E_A, E = activation energy for the reaction, *J/kmol.*

f_{v0} = fraction of volatiles initially present in the particle, -

g = gravitational acceleration, (m/s^2)

G_o = linear momentum, *Nm*

G_k = the generation of $k = \upsilon(\frac{\partial u_j}{\partial X_i} + \frac{\partial u_i}{\partial X_j})\frac{\partial u_j}{\partial x_j}$

G_b	=	the generation due to buoyancy $= -g_i \frac{\upsilon}{\rho\sigma_h}\frac{\partial\rho}{\partial X_i}$
GCV	=	Gross Calorific Value, *MJ/kg*
h	=	gas convectivity, *W/m² K*
i, j k	=	unit vectors, -
k	=	turbulent kinetic energy, *m²/s²*
k	=	kinetic rate, *s⁻¹*
lpm	=	litre per minute, *m³/min*
M_i	=	molecular weight of species *i* (*kg/kmol*)
m_p	=	particle mass, *kg*
m_r	=	mass fraction of a particular reactant *R*, -
m_P	=	mass fraction of any product species *P*, -
m_{p0}	=	initial of particle mass, *kg*
Nu	=	Nusslet number, -
P	=	the static pressure (gauge) which allows for pressure variationsover the nozzle cross-section owing to centrifugal forces, *Pa*
PVC	=	Precessing Vortex Core
Pr	=	Prandtl number of the continuous phase ($c_p\mu/k\infty$)
ppm	=	part per million
R	=	Universal Gas Constant, 8314 *kN/kg mol K*
RFZ	=	Reverse Flow Zone
Re_D	=	Reynolds number based on the particle diameter and the relative velocity, -
S	=	swirl number, -
S_{mx}	=	the rate of increase of x-momentum due to sources, *Nm*
S_b	=	stoichiometric of oxidant, -
S'_h	=	the source term due to participations of the gas phase in radiation heat Transfer, -
t	=	time, *s*
T	=	Temperature, *K*
TKE	=	Turbulence Kinetic Energy, *m²/s²*
$\bar{u}$	=	mean (time average) of velocity, *m/s*
u_I	=	fluctuation of velocity, *m/s*
U	=	axial velocity, *m/s*
W	=	the velocity tangent to a circle centered on the axis, *m/s*
V	=	vector velocity field in the Cartesian space
x,y, z	=	axes

Greek Letters

α_k, α_e	=	the inverse effective Prandtl numbers for k and e, respectively,
ε	=	dissipation rate, (m^2-s/s^2)
ε_p	=	Particle emmisivity, -
ϕ	=	equivalence ratio, -
η_{CE}	=	combustion efficiency, *%*
φ	=	swirl-vane angle, *radians*
λ	=	excess air ratio, -
μ_t	=	Turbulent viscosity, *m²/s*

μ_{mol} = molecular viscosity, m^2/s
ν = viscosity, m^2/s
$\nu'_{i,k}$ = molar stoichiometric coefficient for species *i*
π = 3.14
θ = radiation temperature, *K*
ρ = density, kg/m^3
σ_h = turbulent Prandtl number, $\frac{\mu_t C_p}{k_t}$
∇ = vector operator
$\overline{\phi_i}$ = time averaged mean value of mole fractions, density or temperature
$1/\rho$ = the true time averaged fluid density

7. REFERENCES

[1] Guillaume, D.W and LaRue, J.C. 1995.*Combustion enhancement using induced swirl.* Experiments in Fluids, Springer-Verlag, 20, 59-60.

[2] Gupta, A.K., Lilley, D.G., Syred, N. 1984. Swirl Flows, Abacus Press,.

[3] Brunner, C.R. 1985. Hazardous Air Emission form Incinerator, Chapman & Hall.

[4] Foster, P..J., Macinnes, J.M. and Scubnell, F. *Isothermal Modelling of a Combustion system with Swirl*. 2000. Combustion Science and Technology, Vol. 155, pp. 51-74.

[5] Magnussen. B. F. and Hjertager, B. H. 1976. *On Mathematical Models of Turbulent Combustion with Special Emphasis on Soot Formation and Combustion.* 16th Symp. (Int'l) on Combustion, Cambridge, MA, pp. 15-20.

[6] Peters, A. A. F. and Weber, R., *Mathemathical Modelling of a 2.25 MW_t Swriling Natural Gas Flame. Part 1: Eddy Break-up Concept for Turbulent Combustion; Probability Density Function Approach for Nitric Oxide Formation.* Combustion Science and Technology, Vol. 110-111, 1995, pp. 67-101.

[7] Spliethoff, H., Greul, U., Maier, H. and Hein, K.R.G. 1995. *A comparison of Air Staging and Reburning*, Proc. Of The Institute of energy Conference, p: 61-70.

[8] Griffiths, A.J. 1999. Beedie, D, Syred, N. and O'Doherty, T., *Experimental and computational investigations of Biomass Combustion in a secondary gasification chamber*. Cardiff University.